PROCEEDINGS OF SPIE

SPIEDigitalLibrary.org/conference-proceedings-of-spie

Effect of hydrogen incorporation on sub-gap density of states in amorphous InGaZnO thin-film transistors

Mattson, George, Vogt, Kyle, Malmberg, Christopher, Cheong, Paul H.-Y., Wager, John, et al.

George W. Mattson, Kyle T. Vogt, Christopher E. Malmberg, Paul H.-Y. Cheong, John F. Wager, Matt W. Graham, "Effect of hydrogen incorporation on sub-gap density of states in amorphous InGaZnO thin-film transistors," Proc. SPIE 11281, Oxide-based Materials and Devices XI, 112811G (5 March 2020); doi: 10.1117/12.2545439

SPIE.

Event: SPIE OPTO, 2020, San Francisco, California, United States

Effect of hydrogen incorporation on sub-gap density of states in amorphous InGaZnO thin film transistors

George W. Mattson[a], Kyle T. Vogt[a], Christopher E. Malmberg[b], Paul H.-Y. Cheong[b], John F. Wager[c] and Matt W. Graham[a]

[a] Department of Physics, Oregon State University, Corvallis, OR 97331, USA;
[b] Department of Chemistry, Oregon State University, Corvallis, OR 97331, USA;
[c] Department of Electrical Engineering and Computer Science, Oregon State University, Corvallis, OR 97331, USA;

ABSTRACT

Amorphous semiconducting transparent oxides like $InGaZnO_4$ (a-IGZO) have a broad distribution of metal and oxygen vacancy defects that determine thin film transistor (TFT) characteristics and impact device metrics such as hysteresis. Here, we demonstrate how hydrogen modifies the density of states (DoS) through a novel on-chip method that spectrally resolves trap concentration in a-IGZO spanning the bandgap. Requiring laser energies continuously tunable from 0.26 to 3.1 eV, this method also employs difference frequency generation to access shallow states near the conduction band. We characterize the effect of hydrogen incorporation on the sub-gap peaks of the DoS of an a-IGZO TFT. Specifically, our data suggests hydrogen hybridizes with both metal and oxygen vacancy defects. These interactions result in a suppression of oxygen vacancy trap sites and a peak shift in the metal vacancy-related region in the sub-gap DoS near the valence band maximum. Temperature dependent, photon energy-dependent hysteresis, and transient defect lifetime measurements further reveal the strong impact of hydrogen concentration on a-IGZO TFT performance germane to current optical display technology.

Keywords: IGZO, hydrogen incorporation, density of states, photocurrent spectroscopy, difference frequency generation, sub-gap defect state, thin film transistor, amorphous oxide semiconductor

1. INTRODUCTION

1.1 Density of states of amorphous a-IGZO TFT

The amorphous oxide semiconductor $InGaZnO_4$ (a-IGZO) has gained widespread adoption in the display technology industry owing to its low-cost solution processibility, high mobility, flexibility and scalability, and high on-off current ratio.[1–5] While devices containing a-IGZO-based thin film transistors (TFTs) have become commonplace, a variety of phenomena such as positive bias stressing (PBS) and negative bias stressing (NBS) induce issues like hysteresis and/or persistent turn-on voltage shifts that remain concerning for industrial applications. A number of experimental and theoretical works have made the case that these issues are related to the presence of the large density of both oxygen vacancy and metal vacancy-related traps in the semiconductor that results from its disordered structure, with these traps occupying intermediate energies within the gap between the a-IGZO conduction band (CB) and valence band (VB).[6–9] However, reliable characterization of the mid-gap density of states (DoS) has remained an experimental challenge due to the $\sim 10^{-6}$ sensitivity required to measure the trap states at these energies.

Further author information: (Send correspondence to G.W.M.)
G.W.M.: E-mail: mattsong@oregonstate.edu

Oxide-based Materials and Devices XI, edited by David J. Rogers, David C. Look, Ferechteh H. Teherani, Proc. of SPIE Vol. 11281, 112811G · © 2020 SPIE
CCC code: 0277-786X/20/$21 · doi: 10.1117/12.2545439

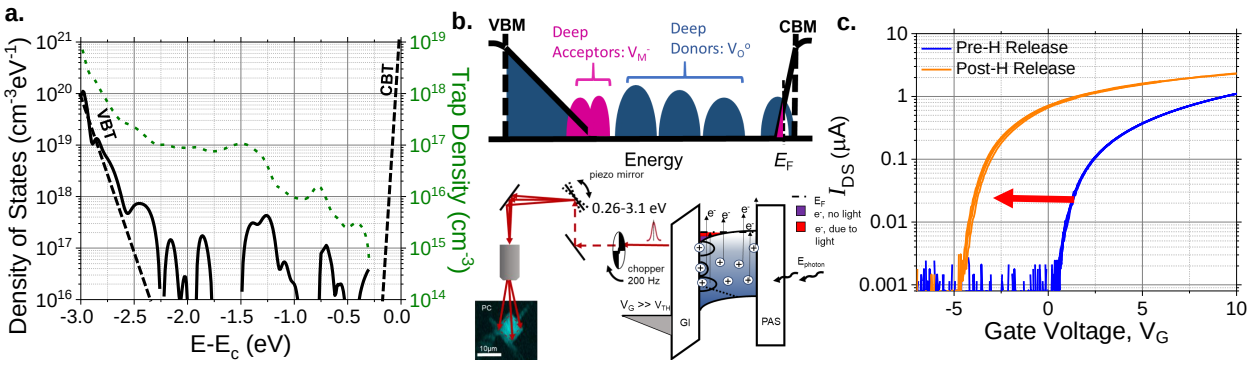

Figure 1. **a.** The experimental trap density and density of states (DoS) of an a-IGZO TFT obtained by the ultrabroadband photoconduction method. The dashed green line shows the trap density and the solid black line shows its derivative with respect to energy, the sub-gap density of states. **b.** (*Upper*) DFT simulation indicates the presence of donor-like (blue) and acceptor-like (magenta) peaks in the a-IGZO sub-gap DoS, near the conduction and valence band edges, respectively. (*Lower left*) Frequency-modulated laser light with photon energies tunable from ~ 0.26 to 3.1 eV is focused onto a diffraction-limited area of the TFT active region. The resulting photoconduction signal is mapped spatially and hyperspectrally to measure the a-IGZO sub-gap trap density. (*Lower right*) The effect of laser illumination on the TFT channel under forward bias. Trapped carriers are excited to the conduction band inducing a photoconduction response which is isolated by via lock-in amplification. **c.** The release of hydrogen into the a-IGZO TFT conducting channel results in a negative shift of 5 V due to the doping of the conduction band with excess carriers.

2. EXPERIMENT AND RESULTS

2.1 Ultrabroadband photoconduction of amorphous semiconductors

A novel on-chip method for measuring the mid-gap density of states of disordered semiconductors like a-IGZO is employed. This ultrabroadband photoconduction (UBPC) technique uses lock-in detection to isolate the small photoconduction ($0.1 - 10$ nA) induced by local laser excitation of an a-IGZO thin film transistor (TFT). In this contribution, we continuously tune laser light over a $0.26 - 3.1$ eV range using mirror-based diffraction-limited focusing on the conducting channel of the TFT. As shown in Figure 1b, the spatial UBPC response is optimized via confocal scanning for uniform and device-characteristic photocurrent. Since the resulting photocurrent maps directly to the total density of traps at a given photon energy, by illuminating and measuring the TFT over band gap, the density of states can be obtained simply by taking the derivative of the trap density with respect to photon energy. Providing the laser energy is tuned with sufficiently fine granularity ($5 - 10$ nm in the visible range), the trap density and DoS are empirically obtained using:[10]

$$N_{Traps} \approx \int_{VBM}^{CBM - E_{Photon}} DoS(E)dE \tag{1}$$

$$\frac{dN}{dE} \approx DoS(CBM - E_{Photon}) \tag{2}$$

Figure 1a contains the experimental trap density and DoS of an a-IGZO TFT obtained through UBPC measurement. Both donor and acceptor-like traps are measured by UBPC, with DoS peaks corresponding to steps in the raw photoconduction signal after lock-in amplifier demodulation of any transfer curve drift. Figure 1b (Upper) shows a simplified picture of the mid-gap DoS as indicated by DFT simulation. Density functional theory (DFT)-based calculations shed additional light onto the character of the states in the a-IGZO mid-gap. A statistically weighted set of unit cells containing the constituent atoms of the semiconductor in all combinations of partial coordination environments were generated and assigned energies after DFT-based structural relaxation. According to this *ab intio* simulation in Vogt et al., states within about 2.0 eV of the CB were associated with donor-like oxygen vacancies (V_O), while the states closer to the VB (> 2.0 eV below CB) were linked to acceptor-like metal vacancies (V_M).[10]

2.2 Impacts of hydrogen diffusion on a-IGZO density of states

One practical novel application of the UBPC method is to gauge how TFT processing conditions and the introduction of impurities modulate the sub-gap DoS peaks in semiconductors like a-IGZO. On account of its small size and diffusive-reactivity, hydrogen is often an unavoidable source of vacancy-induced reliability effects in a variety of semiconductors including a-IGZO. A number of theoretical and experimental works have explored the effect of hydrogen incorporation on a-IGZO TFT performance and reliability,[9,11–13] but the development of the UBPC technique allows for a more direct measurement of the effect of hydrogen incorporation on an a-IGZO TFT DoS.

In order to determine the effect of hydrogen on an a-IGZO TFT, we measured the DoS of a control a-IGZO TFT and compared it against an identically grown sample that was subsequently capped with a hydrogen-rich top-layer. Figure 2 shows the density of states of the a-IGZO TFT with an H-rich layer (blue) versus a control device (black). The DoS shows very little difference between the control and H-rich layer capped device, consistent with minimal H diffusion into the device at room temperature.

The sample with the hydrogen-rich layer was then heated to approximately 200° C above room temperature for two hours to cause diffusion of hydrogen from the H-rich layer into the TFT. It was then cooled back to room temperature to allow the mobile hydrogen to settle and interact with defects in the channel. As shown in Figure 1c, hydrogen diffusion into the a-IGZO TFT ridgidly shifts the device turn-on voltage negative by ~ 5 V. The sub-gap DoS was also strongly impacted by hydrogen incorporation. Figure 2a shows a substantial (~ 2X) suppression in the mid-gap DoS within 2.0 eV of the conduction band and similar relative enhancement in the DoS region adjacent to VB Urbach tail.

Figure 2 reveals the impact of hydrogen incorporation on both the DoS and trap density. Hydrogen undergoes a diffusion-reaction in a-IGZO which passivates donor-like V_O traps within 2.0 eV of the CB and replaces the near-VB acceptor-like V_M traps with OH^- sites with a different energy and absorption cross-section. The V_O trap suppression also enhances a state about 0.4 eV above the VBM suggesting possible hydrogen to metal (H-M) bonding. A control device was subjected to a comparable heating treatment but did not exhibit noticeable changes in either the device transport characteristics or the DoS, suggesting that the changes observed in the DoS are directly attributable to hydrogen diffusing into the a-IGZO TFT channel from the H-rich layer rather than some extraneous device heating effect.

2.3 Temperature-induced DoS shift in a-IGZO TFT

The effect of temperature on an *as-grown* (control) a-IGZO TFT provides additional insight into the contribution of hydrogen to the DoS peak located near 0.7 eV above the VB (2.3 eV from the CB). Figure 3a shows that upon cooling the TFT down to 140 K, we observe a strong enhancement in photoconductivity localized to the V_M region of the spectrum. The photoconduction associated with this peak decreased monotonically with increasing temperature. Figure 3b highlights that peak lineshape changes from Gaussian-like to nearly flat once heated to maximum temperature of 350 K. The temperature trend in the photoconduction data is consistent with the idea that hydrogen becomes more labile as temperature increases and is able to interact more with the V_M sites related to this peak. This interaction (O-H bonding) suppresses the V_M region peak-maximum, suggesting more delocalized carriers. An accompanying doping effect on the CB is expected to be consistent with a negative shift in the turn-on voltage with increasing temperature (Figure 3b, left inset).

3. DISCUSSION

3.1 Hydrogen diffusion-reaction in a-IGZO

The effect of hydrogen incorporation on a-IGZO TFTs has been the subject of substantial theoretical and experimental work.[9,11,12] Hosono and Robertson have suggested that hydrogen interacts as an H^- ion.[11,12] According to this model, H_2 interacts with electrons in a filled donor-like oxygen vacancy trap site and creates transient H^- ions, which can then bond to the undercoordinated metal atoms at the V_O vacancy according to:

$$H_2 + {V_O}^0 \rightarrow [2H^- - V_O^{2+}]^0 \tag{3}$$

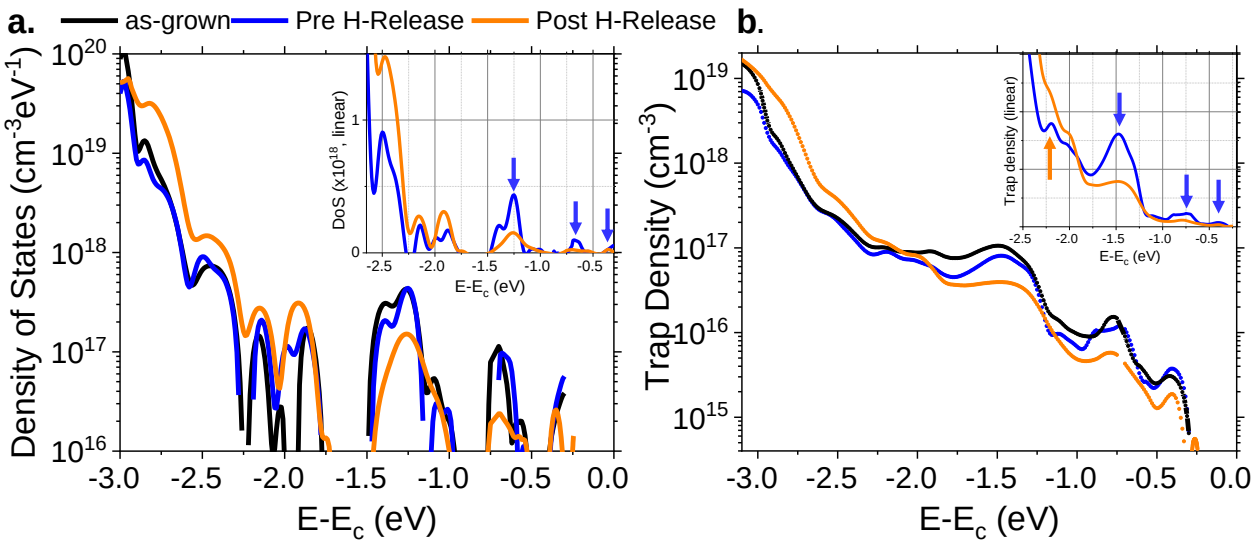

Figure 2. **a.** The experimental density of states (DoS) for the *as-grown* a-IGZO (black) TFT, a-IGZO TFT post-deposition of a hydrogen-rich encapsulation layer (blue), and a post-thermal hydrogen release a-IGZO TFT (orange). Hydrogen is released from the H-rich layer as molecular hydrogen and moisture (H_2O). This can passivate deep-donor V_O trap states through metal hydrogen (M-H) bonding and oxygen transport, with the former resulting in an enhanced M-H bonded contribution to the DoS state near the VBM. The hydrogen interaction with metal vacancy V_M sites may further form an OH^- bond. The latter proposed mechanism is supported by DoS peak-height change in the near-VB DoS. (*Inset*) DoS (linear scaling) highlights the suppression of mid-gap deep-donor peaks and the enhancement of near-VBM M-H related states after H-release. **b.** The trap density vs. photon energy suggests the trap density for the hydrogen-incorporated TFT is lower all throughout the donor-like region of the mid-gap, which is consistent with the suppression of these traps as a result of hydrogen incorporation. (*Inset*) The trap density on a linear scale reveals that H incorporation strongly suppresses the density of sub-gap V_O and V_M traps while enhancing the metal-hydrogen peak density near the VB tail.

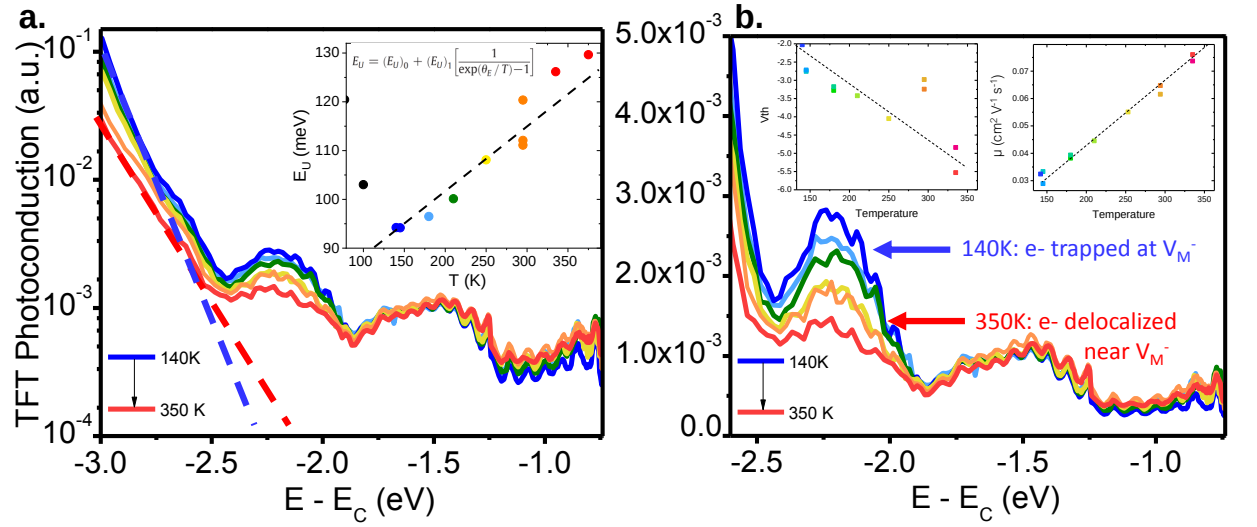

Figure 3. **a.** The photoconduction spectrum of an a-IGZO TFT upon heating from 140 to 350 K. At 140 K, electrons are strongly localized in the metal vacancy traps, resulting in a sharply peaked Gaussian-lineshape. Increasing temperature enhances electron delocalization resulting in a step-like lineshape profile in the photoconduction spectrum. (*Inset*) The valence band Urbach tail energy increases linearly as temperature increases according to established model[14] shown by the dashed line fit. **b.** The TFT photoconduction on a linear scale. (*Inset, left*) The threshold voltage shifts left with increasing temperature. (*Inset, right*) The TFT carrier mobility approximately increases linearly with temperature.

The $[H - V_O]$ complex written above is nothing more than a metal-hydrogen (M-H) bond, which DFT results have suggested lies approximately 0.4 eV above the VB in a-IGZO.[9,12] This model is consistent not only with the suppression of mid-gap oxygen vacancy peaks observed in our experimental DoS as a result of hydrogen incorporation, but also with the enhancement of the DoS near the VB.

An alternative scenario is possible where where hydrogen can diffuses into a-IGZO as moisture (H_2O). Here we must consider another reaction suppressing V_O-related traps. In oxides, the hydrogen atoms in diffusing H_2O molecules act as if they are completely contained within the electron cloud of O atoms. As a result the ionic radius is similar to that of an O atom, but it has a larger diffusion coefficient.[15–17] This suggests that H_2O may react similarly to an oxygen molecule (i.e. by passivating an oxygen vacancy) while accessing traps not previously accessed by oxygen diatoms in the bulk. The diffusion of oxygen-like H_2O molecules allows for an additional reaction that similarly passivates V_O molecules while maintaining charge neutrality in the semiconductor:

$$V_O{}^0 + [H^+ - O^{2-} - H^+] \rightarrow H_2 \tag{4}$$

In situations where the O_2 content of or H_2O diffusion into the TFT is not explicitly controlled for, as was the case for the devices in this study, this reaction can supplement the metal-hydrogen model in explaining why the oxygen vacancy-related trap density decreases with hydrogen incorporation. Li et al. have suggested a similar interaction in ZnO in which both the oxygen and hydrogen atoms from an H_2O molecule passivate different oxygen vacancy sites simultaneously.[11]

Regardless of whether H or O atoms passivate the vacancy, it is a charge neutral reaction in either case and therefore does not explain why hydrogen incorporation induces a large negative threshold voltage shift in Fig. 1c. This shift is driven by hydrogen interaction with metal vacancy states near the VB to form a hydrogen metal vacancy complex (or OH^- state), a process that releases free carriers into the CB:

$$H + V_M^{2-} \rightarrow [V_M - H]^- + e^- \tag{5}$$

Because the metal vacancy is passivated by hydrogen bonding with undercoordinated O atoms, the $[V_M - H]^0$ complex is effectively the same as a donor-like OH^- state, suggesting:

$$O^{2-} + H \rightarrow OH^- + e^- \tag{6}$$

The negative shift in the turn-on voltage and the changes observed in the near-VB a-IGZO TFT DoS peaks are the product of V_M sites being replaced by OH^- sites that have both different state energy and absorption cross section lineshape. As molecular hydrogen interacts with the metal vacancy traps just below 2.0 eV from the conduction band, it may convert such trap sites into OH^- complex sites, doping the CB with excess free carriers while simultaneously suppressing traps in the metal vacancy region. The $[V_M - H]$ complex (OH^- creation) therefore may serve as the mechanism for the negative turn-on voltage shift observed.

3.2 Trapping lifetimes and capture cross section

The decay of the photocurrent signal of an a-IGZO TFT at any given photon energy depends on which types of vacancies get photoexcited. Specifically, deep-donor and deep-acceptor traps intrinsically give different electron capture cross sections owing to their local charge. For instance, an empty deep-donor trap is positively charged and exerts a Coulombic force on a negatively charged free carrier whereas an empty deep-acceptor trap is neutral.[10] As highlighted in the inset of Fig. 4a, these distinct capture cross sections give distinct contributions to the transient photocurrent fall time of the TFT. In the mid-gap region the dominant trap species are oxygen vacancy deep-donors and show a characteristic fall time of about ~ 0.4 ms over the entire region. Towards the VB, the net fall time begins to take on the characteristics of the V_M acceptor-like vacancies in this region, which have a fall time on the order of ~ 1 ms.

Figure 4a suggests that hydrogen incorporation does not have a large impact on the transient photocurrent fall times measured within ~ 2.3 eV of the CB. The slightly longer fall times observed in this oxygen vacancy energy range after H-release suggest a weak dependence of the ensemble fall time on the total number of traps, with the

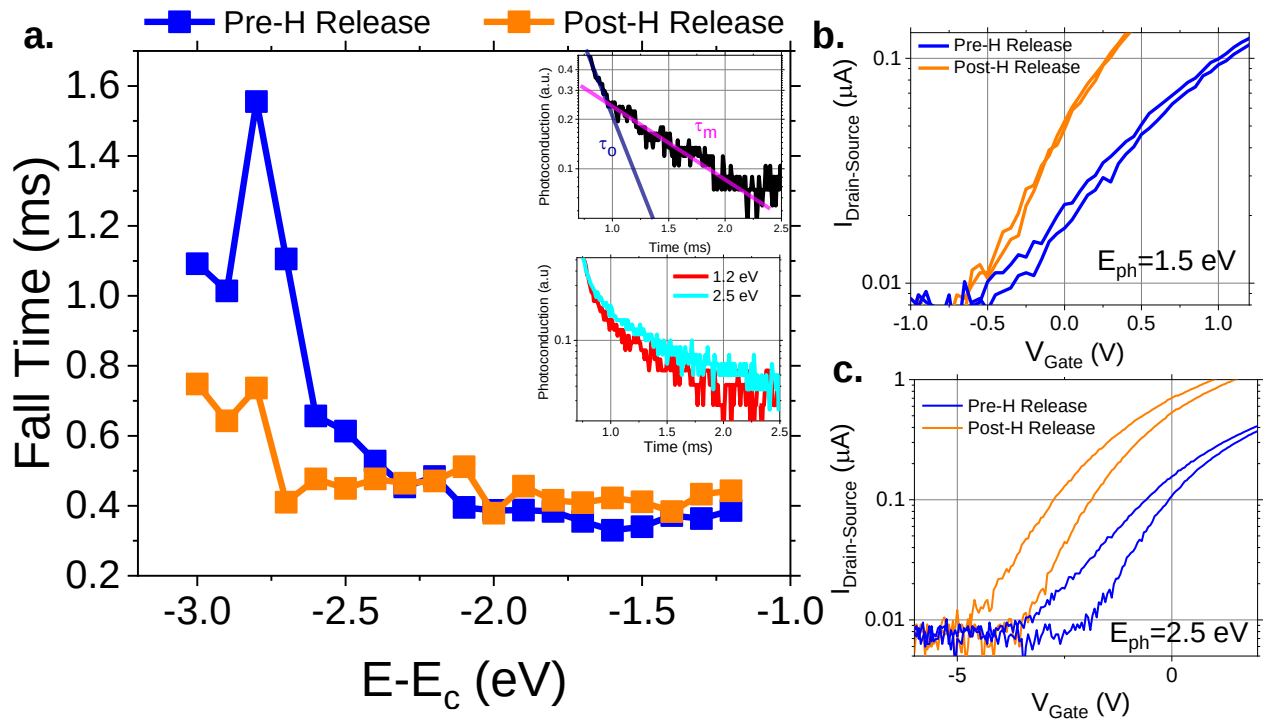

Figure 4. **a.** The photoconduction signal falls in a multiexponential fashion, with a characteristic fall time that depends on the trap species predominating at the photoexcitation energy. While hydrogen does not strongly affect the fall time in the deep-donor oxygen vacancy region, hydrogen presence results in substantially faster fall times in the deep-acceptor metal vacancy region. (*Inset, upper*) The transient photoconduction signal in a-IGZO yields at least two distinct exponential decays times, with a donor-like lifetime on the scale of $\sim$ 0.1 ms and an acceptor-like lifetime on the scale of $\sim$ 1 ms. (*Inset, lower*) The multiexponential nature of the photoconduction signal decay in a standard a-IGZO TFT results in a longer decay for photon of 2.5 eV than for 1.2 eV owing to the high-density of acceptor-like metal vacancy traps with slower electron capture times. **b.** The illuminated transport curve for a-IGZO at a photon energy of 1.5 eV indicates that photon-induced hysteresis is reduced in the post-hydrogen incorporation TFT. c. By contrast, using a photon energy of 2.5 eV, the illumination-induced hysteresis is more severe for the post-hydrogen incorporation sample compared to the *as-grown* a-IGZO TFT.

smaller number of V_O traps in the post H-release device resulting in a longer effective capture time. In contrast with the V_O range fall times, the ensemble fall times closer to the VB tail exhibit a large dependence on H incorporation, with the post-H release sample exhibiting substantially smaller fall times in this region compared to the control device. This divergence is consistent with a shift in the local trap-coordination environment rather than just absolute numerical density. Since the OH^- state that replaces V_M traps is positively charged, it may exert a Coulombic force on CB carriers causing its capture time to become closer to that of a V_O vacancy than a V_M vacancy. Accordingly, when the V_M traps are occupied by hydrogen, the ensemble fall times remain relatively similar through the mid-gap energy range.

Photon energy-dependent hysteresis is also connected to the interplay between hydrogen and the mid-gap trap states, as evidenced by the illuminated device transfer curves in Figure 4b and 4c. As the photon-induced hysteresis in a-IGZO may depend on the energy of the local traps states, the reduction of the mid-gap V_O traps after hydrogen incorporation may lessen the positive illuminated bias induced hysteresis. Similarly, if the states near the VB are enhanced after hydrogen-incorporation, the photon-induced hysteresis in Fig. 4c is wider with a larger negative turn-on voltage compared to the pre-H release device. A full treatment of the effect of hydrogen incorporation on a-IGZO TFT reliability phenomena is beyond the scope of this conference proceeding, but the dependence of illumination-induced hysteresis on hydrogen-modulated peaks in the DoS provides preliminary data and models that unambiguously connect hydrogen incorporation with a-IGZO TFT device reliability.

4. EXPERIMENTAL SETUP

Multiple tunable lasers were employed to obtain the necessary range for UBPC. For the visible range ($0.7 - 3.1$ eV), a Fianium SC-400 supercontinuum laser was coupled to a Photon etc. Laser Line Tunable Filter which enabled rapid iteration over the visible range at $5 - 10$ nm increments. To obtain photocurrent data below 0.7 eV, a Coherent Chameleon Ti:Sapphire laser was employed in concert with an A.P.E. Compact Optical Parametric Oscillator (OPO). Mid-IR laser light was generated via a nonlinear frequency mixing technique known as difference frequency generation.[18,19] The signal and idler beam outputs from the OPO were aligned spatially and temporally and focused on an $AgGaS_2$ crystal to generate coherent radiation in the $0.26 - 0.31$ eV range. For all illumination regimes, a ThorLabs 40X reflective objective focused the laser light onto a diffraction-limited region of the a-IGZO TFT and the spot location in the TFT channel was optimized with a piezoelectric mirror-based confocal scanning setup providing simultaneous spatial maps of both photocurrent and back reflection. To separate the UBPC photocurrent response from a drifting device background, a Zurich Instruments HF2LI Lock-In Amplifier was synchronized to a phase-locked optical chopper operating at 200 Hz.

5. CONCLUSION

The widespread adoption of a-IGZO TFTs in thin film display technology strongly motivates the characterization of its mid-gap density of states. Using our ultrabroadband photocurrent method,[10] we experimentally obtained the density of states for a-IGZO TFTs under *as-grown*, and pre/post-release conditions of a hydrogen-rich layer. This systematic incorporation of hydrogen both rigidly shifted the device transfer curves by ~ -5 V and fundamentally altered the sub-gap density of states. Specifically, we observed the suppression of oxygen vacancy-related peaks within 2.0 eV of the CB, which was anti-correlated to a peak enhancement in the near-VBM region of the DoS consistent with a M-H bonding model. We propose two possible mechanisms through which hydrogen replaces V_O sites: M-H bonding (a charge neutral interaction) and H_2O passivation of V_O traps via transporation of O^{2-} ions to the trap site (also charge neutral). H interaction with V_M sites leads to suppression of these traps due to O-H interaction, which shifts the transfer curve negatively by introducing carriers into the CB. Temperature-dependent density of states data taken from $140 - 350$ K provides further evidence that hydrogen forms a donor-like hydroxyl state ($[V_M - H]$ complex) with metal vacancy sites. Specifically, hydrogen becomes more labile in a-IGZO with increasing temperature to account for the observed decrease in state density. Lastly, transient photocurrent lifetime measurements also support that hydrogen may replace metal vacancies near the VB. This is indicated by a large change in the trap-dependent photocurrent fall times after hydrogen incorporation. To close the loop, the photon energy-dependent hysteresis relates hydrogen incorporation to TFT reliability, motivating careful control of hydrogen to improve amorphous semiconductor TFT performance.

REFERENCES

1. K. Nomura, H. Ohta, A. Takagi, T. Kamiya, M. Hirano, and H. Hosono, "Room-temperature fabrication of transparent flexible thin-film transistors using amorphous oxide semiconductors," *Nature* **432**(November), p. 488, 2004.
2. T. Kamiya, K. Nomura, and H. Hosono, "Present status of amorphous In-Ga-Zn-O thin-film transistors," *Science and Technology of Advanced Materials* **11**(4), 2010.
3. S. R. Thomas, P. Pattanasattayavong, and T. D. Anthopoulos, "Solution-processable metal oxide semiconductors for thin-film transistor applications," *Chemical Society Reviews* **42**(16), pp. 6910–6923, 2013.
4. Y. Shin, S. T. Kim, K. Kim, M. Y. Kim, S. Oh, and J. K. Jeong, "The Mobility Enhancement of Indium Gallium Zinc Oxide Transistors via Low-temperature Crystallization using a Tantalum Catalytic Layer," *Scientific Reports* **7**(1), pp. 1–10, 2017.
5. J. Troughton and D. Atkinson, "Amorphous InGaZnO and metal oxide semiconductor devices: An overview and current status," *Journal of Materials Chemistry C* **7**(40), pp. 12388–12414, 2019.
6. J. Robertson and Y. Guo, "Light induced instability mechanism in amorphous InGaZn oxide semiconductors," *Appl. Phys. Lett.* **104**, p. 162102, Apr. 2014.
7. J. H. Kim, E. K. Park, M. S. Kim, H. J. Cho, D. H. Lee, J. H. Kim, Y. Khang, K. C. Park, and Y. S. Kim, "Bias and illumination instability analysis of solution-processed a-InGaZnO thin-film transistors with different component ratios," *Thin Solid Films* **645**(March 2017), pp. 154–159, 2018.
8. J. Jia, A. Suko, Y. Shigesato, T. Okajima, K. Inoue, and H. Hosomi, "Evolution of Defect Structures and Deep Subgap States during Annealing of Amorphous In-Ga-Zn Oxide for Thin-Film Transistors," *Physical Review Applied* **9**(1), p. 14018, 2018.
9. A. de Jamblinne de Meux, G. Pourtois, J. Genoe, and P. Heremans, "Defects in Amorphous Semiconductors: The Case of Amorphous Indium Gallium Zinc Oxide," *Phys. Rev. Applied* **9**, p. 054039, May 2018.
10. K. T. Vogt, C. E. Malmberg, J. C. Buchanan, G. W. Mattson, G. Mirek, D. B. Fast, P. H. Cheong, J. F. Wager, and M. W. Graham, "Ultrabroadband Density of States of Amorphous In-Ga-Zn-O," *Materials Science* , pp. 1–21.
11. H. Li, Y. Guo, and J. Robertson, "Hydrogen and the Light-Induced Bias Instability Mechanism in Amorphous Oxide Semiconductors," *Sci Rep* **7**, p. 16858, Dec. 2017.
12. J. Bang, S. Matsuishi, and H. Hosono, "Hydrogen anion and subgap states in amorphous In–Ga–Zn–O thin films for TFT applications," *Appl. Phys. Lett.* **110**, p. 232105, June 2017.
13. Y. Nam, H. O. Kim, S. H. Cho, C. S. Hwang, T. Kim, S. Jeon, and S. H. Ko Park, "Beneficial effect of hydrogen in aluminum oxide deposited through the atomic layer deposition method on the electrical properties of an indium–gallium–zinc oxide thin-film transistor," *Journal of Information Display* **17**(2), pp. 65–71, 2016.
14. R. C. Rai, "Analysis of the Urbach tails in absorption spectra of undoped ZnO thin films," *Journal of Applied Physics* **113**, p. 153508, Apr. 2013.
15. R. H. Doremus, *Diffusion of Reactive Molecules in Solids and Melts*, 2001.
16. R. H. Doremus, "Diffusion of water in silica glass," *Journal of Materials Research* **10**(9), p. 2379–2389, 1995.
17. J. E. Shelby, "Molecular diffusion and solubility of hydrogen isotopes in vitreous silica," *Journal of Applied Physics* **48**(8), pp. 3387–3394, 1977.
18. R. W. Boyd, *Nonlinear Optics, Third Edition*, Academic Press, Inc., USA, 3rd ed., 2008.
19. G. Stibenz, M. Beutler, I. Rimke, V. Badikov, D. Badikov, and V. Petrov, "Femtosecond mid-IR difference-frequency generation in BaGa2GeSe6 from a 40 MHz optical parametric oscillator pumped at 1035 nm," *2018 Conference on Lasers and Electro-Optics, CLEO 2018 - Proceedings* **33**(11), pp. 7–11, 2018.